MATHEMATICAL BIOSCIENCES
AND ENGINEERING
Volume **8**, Number **4**, October **2011**

doi:10.3934/mbe.2011.8.1061

pp. **1061–1083**

A MATHEMATICAL MODEL OF THE COMPRESSION OF A SPINAL DISC

Matthias Ngwa

Calgary Board of Education
Calgary, AB T2G 2L9, Canada

Ephraim Agyingi

School of Mathematical Sciences
Rochester Institute of Technology, Rochester, NY 14623-5801, USA

(Communicated by Qing Nie)

Abstract. A model is developed of the stress-strain response of an intervertebral disc to axial compression. This is based on a balance of increased intradiscal pressure, resulting from the compression of the disc, and the restraining forces generated by the collagen fibres within the annulus fibrosus. A formula is derived for predicting the loading force on a disc once the nucleus pressure is known. Measured material values of L3 and L4 discs are used to make quantitative predictions. The results compare reasonably well with experimental results.

1. **Introduction.** The intervertebral disc is prone to ruptures and degenerative processes [26]. Mechanical stress applied to the disc appears to accelerate the development of degenerative changes. There is thus considerable interest in understanding how the application of different loadings to the spine affects the stresses that it experiences [27].

In a normal unloaded disc, a small but positive pressure is present within the nucleus pulposus at rest and this pressure increases when loads are applied to the spine [17, 22, 23, 28, 36]. When the spine is axially compressed, the force applied to the intervertebral disc is balanced by an increase in this pressure [19, 23]. This pressure, which does not vary with location within the nucleus pulposus [22, 23], places the fibres of the annulus in tension, so that they are stretched, leading to annular bulging [10]. The objective of this paper is to develop a model that describes this behaviour and in particular to predict how the pressure varies with the load transmitted through the spine. To do this we shall assume that the vertical displacement of the discs is specified. Using this as a parameter we are then able to make predictions about the pressure in the nucleus pulposus, the load transmitted by the disc as well as the sideways displacement of the annulus fibrosus.

We use the model to make a comparison with the experimental results of Nachemson and Morris [25]. They measured the pressure in the nucleus pulposus and the

2000 *Mathematics Subject Classification.* Primary: 74F10, 74L15, 92C10; Secondary: 92B05.
Key words and phrases. Intervertebral disc, axial compression, intradiscal pressure, fibre displacement.

load carried by the body. We are able to predict the loading from the pressure measurement and compare it with the measured load.

2. **Description of intervertebral disc.** There are 23 intervertebral discs in humans between the bodies of adjacent vertebrae from the second cervical vertebra to the sacrum. They are thicker in the lumbar region, where movements of the spine are greatest, than in other regions of the vertebral column, with the fifth lumbar disc most commonly the largest [32]. The intervertebral disc connects the cartilaginous endplates of two adjacent vertebral bodies and its shape corresponds to that of the vertebral bodies. It is made up of two distinct parts: the nucleus pulposus and the annulus fibrosus, as depicted in Fig. 1.

The nucleus pulposus is located in the centre of the disc. It is bounded above and below by the superior and inferior cartilaginous endplates and on its periphery by the annulus fibrosus. It is composed of a concentrated proteoglycan solution containing randomly distributed collagen fibres. The collagen network of the nucleus has been shown to interconnect with that of the inner annulus [16] and some connections with the end-plate have been observed [9]. The nucleus functions as a gel, distributing forces of compression and tension equally to all parts of the annulus [1, 29].

The annulus fibrosus is quite distinct from the nucleus and forms the outer boundary of the disc. It contains a series of 15 to 25 concentric layers (lamellae) of fibrous tissue [20]. The fibres within each lamella are arranged in a helicoid manner, and have two well-defined axes of orientation. The fibres in each lamella run in a single direction, alternating from the previous one and aligned at an approximate constant angle of 30^o to the horizontal axis according to Vijay and Weinstein [35]. According to Bayliss and Johnstone [7], they are oriented at an angle varying between 20^o–50^o to the horizontal axis. By this means the annulus is able to withstand strain in any direction [21]. The space between the collagen fibre framework is filled with proteoglycan, which in turn attracts and holds large amounts of water [12]. In the fibrocartilaginous inner annulus (area adjacent to the nucleus), the fibres terminate in the cartilaginous end-plate which is a thin layer of hyaline cartilage on the surface of the vertebra. In the outer region the fibres are connected directly to the osseous tissue of the vertebral body where they are known as Sharpey's fibres [7]. The fibres constitute 16–19% of the annulus volume [19, 35]. A radial variation in biochemical content exists within the disc, with an increasing amount of collagen, and decreasing amounts of water and proteoglycan towards the periphery of the annulus [5, 14, 15]. The collagen fibre content is also dependent on the level of the disc. The stress-strain behaviour of the collagen fibres has been measured and it is observed to vary both with level and with their radial and azimuthal position within a disc [19].

3. **Description of the model.** A good number of analytic or geometric and finite element models have been developed to describe the structural response of intervertebral discs. Most of the previous existing models of the intervertebral disc have modelled the nucleus pulposus as an incompressible, inviscid fluid [8, 18, 26, 34], and we also assume this in our model. The annulus fibrosus has been assumed to be a homogeneous material with either isotropic [34] or orthotropic [8] properties. In [18], Galante is noted to have shown experimentally that the annulus is nonhomogeneous and anisotropic and exhibits hardening stress-strain characteristics. The cartilaginous end-plate has been considered as an isotropic, homogeneous elastic

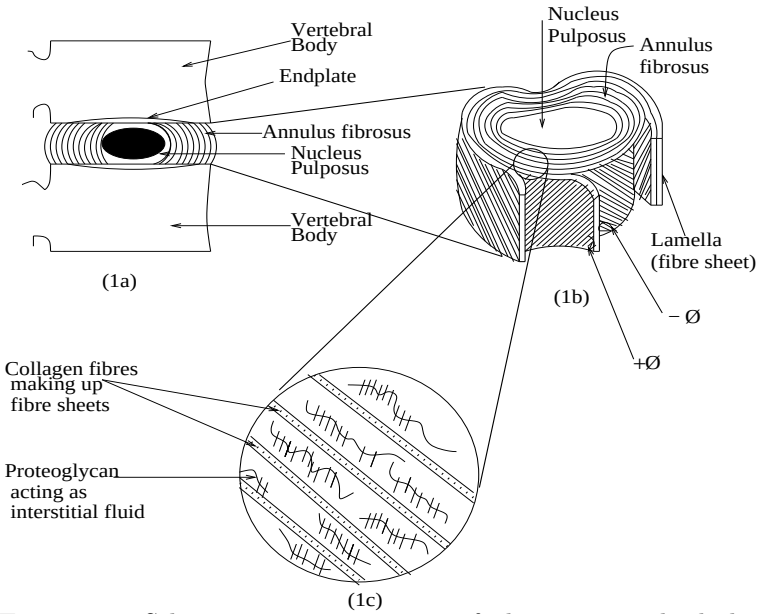

FIGURE 1. Schematic representation of the intervertebral disc showing collagen fibres in alternating layers within the annulus. (1a) Disc location between vertebrae; (1b) Cut out section of disc showing annulus fibrosus layers; (1c) Cross-section of the internal structure of the annulus fibrosus.

linear material [8, 34] while in [34], Spilker et *al.* assumed that the vertebral body is nearly rigid. In most of the previous models of the intervertebral disc, especially the finite element studies, [8, 18], no clear distinction is made between the fibres and the matrix of ground substance, and they are assumed to have the same displacement field. However, this would generate tangential forces within the matrix of ground substance. This is not entirely consistent with the fact that the ground substance principally consists of proteoglycan and water, which in the nucleus pulposus acts as a liquid. Because of this we believe it is necessary to distinguish between the two phases of the annulus fibrosus. We treat the fibres as unbroken sheets (lamellae) which are able to withstand tensile forces along the lengths of the fibres, and the ground substance as a passive liquid that separates the sheets. This will lead to a different set of equations to the normal composite material model. The displacement field of the fibres will no longer be divergence free since local increase in fibre density can be compensated by local reduction in the liquid density. We gain an additional dynamic equation since the liquid ground substance is only able to generate a normal force on each fibre sheet. We assume that the sheets are evenly distributed with radial distance and that the fibres all have the same size and are laid out with the same even spacing within the different sheets. This assumption of uniformity is not necessary for the success of the model but we have no quantitative measure of the variation of these quantities and it is the simplest assumption to make.

4. **Model formulation.** We now develop equations by comparing the disc in two states, the initial state where it is under no loading and the final state where it

is under a loading W. We assume that in both cases the intervertebral disc is axisymmetric about the spinal (vertical) axis. The initial state is illustrated in Fig. 2. We assume that in this state the fibres lie on helices of constant radius that are inclined at fixed constant angles of $+\phi$ or $-\phi$ to the horizontal (perpendicular to the spinal axis) [35], alternating from sheet to sheet. We denote the height of the disc by $2L$ and the inner and outer radii of the annulus fibrosus by a and b, respectively. We assume that a, b and L are comparable in magnitude.

Note that in the initial state the fibres are already stretched and under tension. This is not a trivial point mathematically since the stress-strain relation is nonlinear in the practical range of interest. Also, as a consequence of the fibre tension, the nucleus pulposus is under an initial pressure P_i. This state needs to be given (known) as part of the description of the problem.

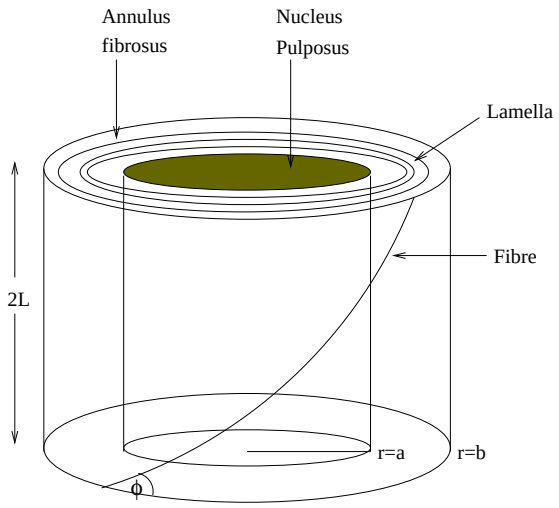

FIGURE 2. Idealized initial state of intervertebral disc

The final state (not illustrated) has the top endplate of the disc displaced downwards by a distance h and the lower endplate displaced upwards by h. Although axisymmetric, the fibres no longer lie on cylinders. Any point on a fibre can be identified by the cylindrical polar co-ordinates (r, θ, z) of its original position or by the cylindrical polar co-ordinates (R, Θ, Z) of its final, deformed position. Since the problem is symmetrical about a horizontal plane through the centre of the disc we take $z = 0$ and $Z = 0$ on that plane. The coordinates are connected by the fibre material displacement functions (u, v, w). One of our main objectives is to determine these displacement fields. They can be defined to be functions of either the original position (r, θ, z) or of the final position (R, Θ, Z). We choose to work with the former. From the axisymmetry of the problem the displacements cannot depend on the azimuthal co-ordinate, so we have

$$R = r + u(r, z), \quad \Theta = \theta + v(r, z), \quad Z = z + w(r, z). \tag{1}$$

Note that (u, v, w) represent only the displacement of the collagen fibres. The continuum phase contained between the fibre sheets has a slightly different displacement field (which we do not actually determine). We neglect any displacement

of the endplate into the vertebrae; in experiments on motion segments [13, 15, 30] this was found to be negligible.

4.1. **The fibre strain equation.** The displacement functions (u, v, w) are field variables, describing the displacement at any point in the domain but not, in themselves, describing the response of any individual fibre. In this section we need to describe the displacement behaviour of single fibres; this can be done by representing the fibres parametrically. In the original state each fibre lies on a helix that can be described by

$$r = q, \quad \theta = s + p, \quad z = qs\tan\phi$$

where q and p identify the fibre, and s distinguishes the points along the fibre. In its displaced location the fibre is described by

$$R = q + u(q, qs\tan\phi),\ \Theta = p + s + v(q, qs\tan\phi),\ Z = qs\tan\phi + w(q, qs\tan\phi). \quad (2)$$

We now obtain an expression for the strain in a given fibre. Consider a typical element of the fibre; the fibre itself is specified by the fixed parameter values q and p and the ends of the element are specified by the parameter values s and $s + ds$. Let the length of this element be denoted by dl'' if it were in an unstretched state, by dl' in its original (partly stretched) state and by dl in its final (fully stretched) state. We use the subscripts $-$ and $+$ to distinguish the co-ordinates of the ends of the element at s and $s + ds$ respectively. Then, in the original state, $r_- = q$, $\theta_- = p + s$, $z_- = qs\tan\phi$ and $r_+ = q$, $\theta_+ = p + s + ds$, $z_+ = q(s + ds)\tan\phi$. The length of this element in this state is given by

$$dl' = q\sec\phi\, ds, \quad (3)$$

and the strain by

$$e_i = \lim_{ds\to 0} \frac{dl' - dl''}{dl''}, \quad (4)$$

where e_i denotes the initial fibre strain. We are taking e_i as a given quantity in the problem formulation so this equation effectively determines the value of dl'', the unknown length of the element in its unstretched state.

Now consider the same element after it has been displaced by the effect of the compression. After the displacement the two end points have co-ordinate values

$$R_- = q + u^*, \qquad \Theta_- = p + s + v^*, \qquad Z_- = qs\tan\phi + w^*,$$

and

$$\begin{aligned} R_+ &= q + u(q, q(s + ds)\tan\phi), \\ \Theta_+ &= p + s + ds + v(q, q(s + ds)\tan\phi), \\ Z_+ &= q(s + ds)\tan\phi + w(q, q(s + ds)\tan\phi), \end{aligned}$$

where the asterisk indicates quantities that are evaluated at the original particle location, e.g., $u^* = u(q, qs\tan\phi)$. The length of the displaced element is

$$dl = \left[q^2\tan^2\phi\, u_z^{*2} + (q + u^*)^2(1 + q\tan\phi\, v_z^*)^2 + q^2\tan^2\phi\,(1 + w_z^*)^2\right]^{\frac{1}{2}} ds. \quad (5)$$

The final strain e is given by the expression

$$e = \lim_{ds\to 0} \frac{dl - dl''}{dl''} = \lim_{ds\to 0} \frac{(1 + e_i)\, dl - dl'}{dl'}. \quad (6)$$

Substituting (3) and (5) into (6), we thus have the following expression for the fibre strain:

$$e = \frac{\cos\phi}{q}\left[(q\tan\phi\, u_z^*)^2 + (q+u^*)^2(1+q\tan\phi\, v_z^*)^2 + \right. \\ \left. + q^2\tan^2\phi\,(1+w_z^*)^2\right]^{\frac{1}{2}}(1+e_i) - 1. \tag{7}$$

Let T denote the tension in a fibre at any point. The constitutive law for the tension is such that it only depends on the local strain of the fibre, i.e. $T = T(e)$. Now we are assuming that the continuous phase is unable to generate tangential forces and hence that it can only push at any point on a fibre in a direction perpendicular to the fibre axis at that point. We shall show later on that, as a consequence of this, the tension along any one fibre takes a uniform value, although this value may vary from fibre to fibre. The restriction that T is a constant implies that e is also uniform along each fibre and so independent of the fibre progress parameter s. In principle, then, $e = e(q,p)$. However, the problem is axisymmetric so e must be independent of p since this parameter only specifies the original azimuthal location of the fibre. Thus $e = e(q)$. We make one last improvement. The final equation is an identity, true for all values of q and s. Hence it remains true if we replace $q \to r$, $qs\tan\phi \to z$. Thus the asterisk (indicating evaluation at $(q, qs\tan\phi)$) is unnecessary and the strain equation can be expressed in the final form

$$e(r) = \frac{\cos\phi}{r}\left[(r\tan\phi\, u_z)^2 + (r+u)^2(1+r\tan\phi\, v_z)^2 + \right. \\ \left. + r^2\tan^2\phi\,(1+w_z)^2\right]^{\frac{1}{2}}(1+e_i) - 1. \tag{8}$$

4.2. **The force balance equations.** We begin by examining a small element of a fibre sheet in its displaced configuration. The element is constructed as a parallelogram with two sides parallel to the fibres and two sides horizontal (constant value of z). See Fig. 3. Let the element length along the fibre be dl and the element

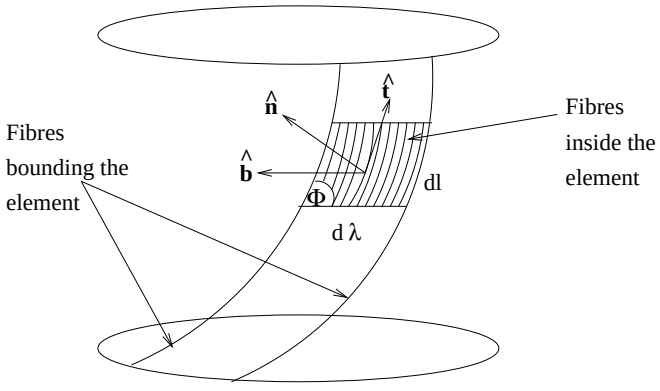

FIGURE 3. Small element of the fibre sheet after displacement

width be $d\lambda$. Let the number of fibres in the element be $\rho_s d\lambda$, where ρ_s is the line density of fibres along the sheet. Let ΔP_s denote the pressure drop from one side of the fibre sheet to the other. We assume from the axial symmetry that the tension T in any fibre is the same as that of any other fibre in the same sheet (and, as

already mentioned, we show later that this distribution is in fact a constant). We now calculate the forces on the element caused by the pressure and the tensions.

We define the forces in terms of the orthogonal basis $(\hat{\mathbf{t}}, \hat{\mathbf{n}}, \hat{\mathbf{b}})$, where $\hat{\mathbf{t}}$ is the unit vector parallel to the fibres in their displaced position, $\hat{\mathbf{n}}$ is the unit vector normal to the displaced fibre sheet, and $\hat{\mathbf{b}}$ is the unit vector perpendicular in a right handed sense to both $\hat{\mathbf{t}}$ and $\hat{\mathbf{n}}$, (so $\hat{\mathbf{b}} = \hat{\mathbf{t}} \wedge \hat{\mathbf{n}}$). It is not immediately obvious but $\hat{\mathbf{n}}$ and $\hat{\mathbf{b}}$ are also the normal and binormal respectively of the individual fibre curves. The force due to the pressure is $\Delta P_s(-\hat{\mathbf{n}}) \times$Area, where the area of the element is $dl\, d\lambda \sin\Phi$. The force due to the tension in the fibres is $(\rho_s\, d\lambda)\left([T\hat{\mathbf{t}}]_{l+dl} - [T\hat{\mathbf{t}}]_l\right)$. The sum of all these forces is zero (since the element is in equilibrium). If we take the limit of all these terms as $dl \to 0$ and $d\lambda \to 0$ (treating the fibre distribution as a continuous variable) we obtain the equation

$$-\Delta P_s \sin\Phi\, \hat{\mathbf{n}} + \rho_s T \frac{\partial \hat{\mathbf{t}}}{\partial l} + \rho_s \frac{\partial T}{\partial l} \hat{\mathbf{t}} = 0. \tag{9}$$

We consider the three components of this equation in turn. First we consider the $\hat{\mathbf{t}}$ component. We note that $\hat{\mathbf{t}}$ is perpendicular to both $\hat{\mathbf{n}}$ and to $\partial\hat{\mathbf{t}}/\partial l$ (the derivative of any unit vector is perpendicular to itself). Thus taking the dot product with $\hat{\mathbf{t}}$ we obtain the component equation

$$\frac{\partial T}{\partial l} = 0. \tag{10}$$

It may be trivially integrated to show that T is constant along the fibre. This result was used earlier to show that $e = e(r)$ only.

The other two components can be obtained by taking the dot products of (9) with $\hat{\mathbf{b}}$ and $\hat{\mathbf{n}}$, respectively, to yield the equations

$$\frac{\partial \hat{\mathbf{t}}}{\partial l} . \hat{\mathbf{b}} = 0, \tag{11}$$

and

$$-\Delta P_s \sin\Phi + \rho_s T \frac{\partial \hat{\mathbf{t}}}{\partial l} . \hat{\mathbf{n}} = 0. \tag{12}$$

We now develop the last of these equations further. We assume that there are a large number of sheets in the disc so that they can be regarded as having a continuum distribution. Specifically, if we examine a small element of a radial line, then the number of sheets that intersect that line can be expressed as $\rho_R\, dR$, where ρ_R is a continuous variable, the linear density of sheets along a radial line. Similarly, we assume that the pressure can be considered to be a continuous variable, rather than changing by discrete amounts at each fibre sheet. Then the gradient of the continuous pressure can be related to ΔP_s by

$$\frac{\partial P}{\partial R} = \lim_{dR \to 0} \left(\frac{(\rho_R\, dR)(-\Delta P_s)}{dR} \right) = -\rho_R \Delta P_s, \tag{13}$$

where the negative sign arises because P decreases with R. Thus combining this with (12) we obtain the normal force balance in continuum form,

$$\frac{\partial P}{\partial R} = -\frac{\rho_R \rho_s}{\sin\Phi} T \frac{\partial \hat{\mathbf{t}}}{\partial l} . \hat{\mathbf{n}}\,. \tag{14}$$

The equations (11) and (14) are expressed in terms of variables and unit vectors that apply at the displaced location, (R, Θ, Z). However, the displacement fields (u, v, w) are functions of the *original* location, (r, θ, z). Thus equations (11) and

(14) must be converted to this co-ordinate system. This is done in the appendix and the results are as follows: Equation (11) becomes

$$r^2\tan^2\phi(r+u)(1+w_z)(1+r\tan\phi\, v_z)w_{zz}-(r+u)^2(1+r\tan\phi\, v_z)^3u_z$$

$$-r^2\tan^2\phi\left[(1+w_z)^2+u_z^2\right]\left[2u_z(1+r\tan\phi\, v_z)+r\tan\phi(r+u)v_{zz}\right]$$

$$+r^2\tan^2\phi(r+u)(1+r\tan\phi\, v_z)u_zu_{zz}=0. \tag{15}$$

We refer to this as the tangential force equation.

Equation (14) becomes

$$(1+w_z)\frac{\partial P}{\partial r}-w_r\frac{\partial P}{\partial z}=-\rho_i\,T(e)\frac{(1+w_z)}{(r+u)(dl/ds)N^2\tan\phi}\times \tag{16}$$

$$\left\{(1+w_z)\left[(r+u)(1+r\tan\phi\, v_z)-r^2\tan^2\phi\, u_{zz}\right]\ +r^2\tan^2\phi\, u_zw_{zz}\right\},$$

where $dl/ds=\left\{u_z^2q^2\tan^2\phi+(q+u)^2(1+v_zq\tan\phi)^2+(1+w_z^2q^2\tan^2\phi\right\}^{\frac{1}{2}}$, $N=\left\{1+2w_z+w_z^2+u_z^2\right\}^{\frac{1}{2}}$ and ρ_i denotes the value of $\rho_r\,\rho_s$ in the initial state. We refer to this as the radial force balance equation.

The basic equations describing the system are thus (10), (15) and (16).

4.3. **Boundary conditions on the problem.** For the displacement functions $(u,\,v,\,w)$, the boundary conditions are

$$u(\pm L)=0,\qquad v(\pm L)=0,\qquad w(\pm L)=\mp h.$$

The pressure before and after axial compression satisfies the following conditions: before compression

$$P=0\quad\text{on}\quad r=b,\quad\text{and}\quad P=\ P_i\quad\text{on}\quad r=a,$$

and after compression they take the form

$$P=0\quad\text{on}\quad r=b,\quad\text{and}\quad P=P_n\quad\text{on}\quad r=a,$$

where P_i must be specified as part of the description of the initial state of the disc and the final final pressure P_n can be calculated from the model.

4.4. **The volume displacement equation.** The volume contained within any fibre sheet of initial radius r remains the same after the superior and inferior surfaces of the disc have been displaced. Hence we have the equation

$$\pi r^2(2L)=\int_{Z=-L+h}^{L-h}\pi R^2dZ=\pi\int_{-L}^{L}(r+u)^2(1+w_z)\,dz. \tag{17}$$

4.5. **Nondimensionalization.** We define a small parameter ε by $\varepsilon=h/2L\ll 1$, where h is the displacement of the endplates and $2L$ is the original height of the disc. We make the model dimensionless in the following way:

$$\begin{aligned} r &= a\tilde{r},\ z=L\tilde{z},\ u=\varepsilon a\tilde{u},\ v=\varepsilon\tilde{v},\ w=\varepsilon L\tilde{w},\ e=\varepsilon\tilde{e}, T=T(\varepsilon E)S(\tilde{e}),\\ P &= \rho_s\,T(\varepsilon E)\tilde{P},\quad dl=L\tilde{dl},\quad \gamma=b/a,\quad\text{and}\quad \alpha=a/L, \end{aligned} \tag{18}$$

where the tildes denote dimensionless variables. We shall work with the assumption that the lengths a and b are comparable to L, so thatγ and α are both $O(1)$

quantities. The scaling for the tension requires further explanation. It is a function of e so as a characteristic magnitude for the tension we use the value T at a representative value of e. However, the variation of T with e is nonlinear so this representative value for e should be characteristic of the final displacement state, and not the initial displacement e_i, at which the value of T is significantly smaller. We have (somewhat arbitrarily) chosen for this purpose the value $e = \varepsilon E$, where $E = \tilde{e_i} + cos^2\phi/a^2$, since this equals $\tilde{e_0}|_{r=a}$, i.e. the value at r = a of the lowest order term in the asymptotic expansion that we derive later. Note also that we have expressed S as a function of $\tilde{e}$. This is because the argument of any dimensionless function, as well as its magnitude, should be an $O(1)$ quantity and e itself, although dimensionless, only varies on the scale of ε. This is equivalent to writing $S = S(e/\varepsilon)$ which physically represents the fact that the tension is very sensitive to e and achieves its typical magnitude when e is only $O(\varepsilon)$. Dropping the tildes for clarity, the model equations (8), (15),(16) and (17), become

$$\begin{aligned}\varepsilon e(r) \quad = \quad & \frac{\cos\phi}{r}\left[(\varepsilon\alpha r\tan\phi\, u_z)^2 + (r+\varepsilon u)^2(1+\varepsilon\alpha r\tan\phi\, v_z)^2\right. \\ & \left. + r^2\tan^2\phi\,(1+\varepsilon w_z)^2\right]^{\frac{1}{2}}(1+\varepsilon e_i) - 1; \end{aligned} \tag{19}$$

$$\begin{aligned} & r^2\tan^2\phi(r+\varepsilon u)(1+\varepsilon w_z)(1+\varepsilon\alpha r\tan\phi v_z)w_{zz} - r^2\tan^2\phi\,\times \\ & \left[(1+\varepsilon w_z)^2+\varepsilon^2u_z^2\right]\left[2u_z(1+\varepsilon r\tan\phi v_z)+\alpha r\tan\phi(r+\varepsilon u)v_{zz}\right] \\ & +\varepsilon\,\alpha^2\,r^2\tan^2\phi\,(r+\varepsilon u)(1+\varepsilon\,\alpha\,r\tan\phi\,v_z)u_zu_{zz} \\ & -(r+\varepsilon u)^2(1+\varepsilon\,\alpha\,r\tan\phi\,v_z)^3u_z = 0; \end{aligned} \tag{20}$$

$$\begin{aligned} & (1+\varepsilon w_z)\frac{\partial P}{\partial r} - \varepsilon w_r\frac{\partial P}{\partial z} = -S(e)\,\frac{\alpha(1+\varepsilon w_z)}{(r+\varepsilon u)(dl/ds)N^2\tan\phi}\,\times \\ & \left\{(1+\varepsilon w_z)\left[(r+\varepsilon u)(1+\varepsilon\alpha\,r\tan\phi\,v_z) - \varepsilon\alpha^2\,r^2\tan^2\phi\,u_{zz}\right]\right. \\ & \left. +\,\varepsilon^2\,\alpha^2\,r^2\tan^2\phi\,u_zw_{zz}\right\}, \end{aligned} \tag{21}$$

and

$$2r^2 = \int_{-1}^{1}(r+\varepsilon u)^2(1+\varepsilon w_z)\,dz, \tag{22}$$

respectively.

4.6. **Perturbation expansion.** We look for an asymptotic solution based on $\varepsilon \to 0$. For this we express the displacement as

$$u \sim u_0 + \varepsilon u_1 + \cdots,$$

with similar expansions for v and w. The leading order term of the volume displacement equation (22) is an identity, $2r = 2r$. At order ε it yields the equation

$$\int_{-1}^{1}(2ru_0 + r^2\frac{\partial w_0}{\partial z})\,dz = 0. \tag{23}$$

The second term can be integrated explicitly and then evaluated, using the boundary condition $w(\pm L) = \mp h$. This condition transforms to $\varepsilon LW(\pm 1) = \mp 2\varepsilon L$, so that

$w_0(\pm 1) = \mp 2$. The equation (23) therefore reduces to

$$\int_{-1}^{1} u_0 \, dz = 2r. \tag{24}$$

We now use this to determine the strain. The dimensionless first order approximation for the strain is given by

$$r\,(e_0(r) - e_i) = \cos^2\phi\, u_0 + \alpha\, \cos\phi \sin\phi\, r^2 \frac{\partial v_0}{\partial z} + r \sin^2\phi\, \frac{\partial w_0}{\partial z}. \tag{25}$$

We integrate over $-1 \le z \le 1$ and apply (24) to obtain

$$e_0 - e_i = \cos^2\phi - 2\sin^2\phi. \tag{26}$$

We see that the change in strain is the difference of two terms. The individual terms can be interpreted as the strains due to the azimuthal and vertical changes in length of the fibres. With the value of $\phi = \pi/6$ quoted in the literature, the change in strain is positive, so the fibres remain under tension. For the interpretation, first suppose that the fibres are entirely radial in orientation (the limit of $\phi \to 0$; a dense coil). Then the compression would create an average radial displacement δ determined from the condition that the volume increase caused by the radial displacement ($circumference \times height \times average\ displacement = 2\pi r(2L)\delta$) is equal to the volume lost by compression of the disc ($area \times total\ displacement = \pi r^2(2h)$) from which it follows that $\delta = \varepsilon\, r$. Then each loop of the coil would be strained by $(2\pi(r+\delta) - 2\pi r)/\ 2\pi r = \varepsilon$. This is a positive strain. Now suppose that the fibres are entirely vertical. Then the strain produced would be $(-2h)/2L = -2\varepsilon$. This is a negative extension and the fibres would slacken. Note that as in (26) the extension for the vertical stretching has a factor of 2 compared to the extension due to the radial stretching. When the fibres are inclined (in a helix) we get a balance of these two effects that depends on the angle of orientation. It is interesting to note that if ϕ exceeds $\arctan(1/\sqrt{2}) \simeq 35^0$ the change in strain would be negative so that the disc would be unstable to small deformations.

Substituting for $e_0 - e_i$ from (26) into (25) we obtain

$$\frac{\cos^2\phi\, u_0}{r} + \alpha\, \cos\phi\, \sin\phi\, r\, \frac{\partial v_0}{\partial z} + \sin^2\phi\, \frac{\partial w_0}{\partial z} = \cos^2\phi - 2\sin^2\phi. \tag{27}$$

Also, with the perturbations of u, w as above, and $P = P_0 + \varepsilon P_1 + \cdots$, $e = e_0 + \varepsilon e_1 + \cdots$, the leading order terms of the tangential and radial equations are

$$\frac{\cos\phi\,(\sin^2\phi + 1)}{r}\, \frac{\partial u_0}{\partial z} + \alpha\, \sin^3\phi\, r\, \frac{\partial^2 v_0}{\partial z^2} - \cos\phi\, \sin^2\phi\, \frac{\partial^2 w_0}{\partial z^2} = 0; \tag{28}$$

$$\frac{\partial P_0}{\partial r} + \frac{\cos^2\phi}{\sin\phi\, r}\, S_0(r) = 0. \tag{29}$$

Integrating equation (29) with respect to r over $[1, \gamma]$ and applying the boundary condition $P_0 = 0$ at $r = \gamma$ we have

$$P_0 = \frac{\cos^2\phi}{\sin\phi} \left(\int_1^{\gamma} \frac{S_0(r)}{r}\, dr \right). \tag{30}$$

We need to solve for the three unknowns u_0, v_0 and w_0 from equations (27) and (28). A third equation is required for this to be done. We are missing an equation because the radial force equation (21) was degenerate and its zero order expansion

did not contain any displacement variables. We find the required equation from the ε order term in the expansion of this equation and it is given by

$$S_0(r)\left[\alpha\left(\cos^2\phi-1\right)\left(\alpha\frac{\partial^2 u_0}{\partial z^2}-\cos\phi\sin\phi\frac{\partial v_0}{\partial z}\right)+\cos^2\phi\left(\cos^2\phi-2\right)r^{-1}\frac{\partial w_0}{\partial z}\right.$$

$$\left.-\cos^4\phi\, r^{-2}\, u_0\right]+e_1\,\cos^2\phi\, S_1(r)r^{-1}+\sin\phi\,\frac{\partial P_1}{\partial r}=0. \tag{31}$$

5. **Solution.** Now we use equations (27), (28) and (31) to solve for the displacement fields u_0, v_0 and w_0. The structures of u_0, v_0 and w_0 permit a similarity solution in simple powers of r. In particular, we assume that

$$u_0=r\,\mathcal{U}(z),\quad v_0=\frac{\mathcal{V}(z)}{\alpha r\sin\phi},\quad w_0=\mathcal{W}(z),$$

so that the equations can then be expressed, respectively, as

$$\cos^2\phi\,\mathcal{U}+\cos\phi\,\frac{\partial\mathcal{V}}{\partial z}+\left(1-\cos^2\phi\right)\frac{\partial\mathcal{W}}{\partial z}=\cos^2\phi-2\sin^2\phi; \tag{32}$$

$$\cos\phi\left(\sin^2\phi+1\right)\,\frac{\partial\mathcal{U}}{\partial z}+\sin^2\phi\,\frac{\partial^2\mathcal{V}}{\partial z^2}-\cos\phi\,\sin^2\phi\,\frac{\partial^2\mathcal{W}}{\partial z^2}=0; \tag{33}$$

and

$$S_0(r)\left[\left(\cos^2\phi-1\right)\left(\alpha^2\,r\,\frac{\partial^2\mathcal{U}}{\partial z^2}-\cos\phi r^{-1}\frac{\partial\mathcal{V}}{\partial z}\right)+\cos^2\phi\left(\cos^2\phi-2\right)r^{-1}\frac{\partial\mathcal{W}}{\partial z}\right.$$

$$\left.-\cos^4\phi\, r^{-1}\,\mathcal{U}\right]+e_1\,\cos^2\phi\, S_1(r)r^{-1}+\sin\phi\,\frac{\partial P_1}{\partial r}=0. \tag{34}$$

Now we integrate (34) over r from 1 to γ. In order to reduce the complexity of the algebra later on, we denote the integral of $S_0(r)\,r^{-1}$ as j_{-1}, that of $S_0(r)\,r$ as j_{+1} and the ratio $(\alpha^2\,j_{+1})/j_{-1}$ as j^2. The P_1 and e_1S_1 terms are both functions of r and generate unknown constants. These can be combined into a single joint constant which we can denote as $-j_{-1}\,k$. We divide the resulting equation by j_{-1} to obtain

$$\left(\cos^2\phi-1\right)\,j^2\frac{\partial^2\mathcal{U}}{\partial z^2}-\cos^4\phi\,\mathcal{U}$$

$$+\cos\phi\,(1-\cos^2\phi)\,\frac{\partial\mathcal{V}}{\partial z}+\cos^2\phi\,(\cos^2\phi-2)\frac{\partial\mathcal{W}}{\partial z}-k=0. \tag{35}$$

With $\cos\phi=c$ and $\sin\phi=\sqrt{1-c^2}$, equations (32), (33) and (35) can be expressed in rational combinations of $\cos\phi$ as

$$c^2\,\mathcal{U}+c\,\frac{\partial\mathcal{V}}{\partial z}+\left(1-c^2\right)\frac{\partial\mathcal{W}}{\partial z}=3c^2-2; \tag{36}$$

$$\left(c^3-2c\right)\frac{\partial\mathcal{U}}{\partial z}+\left(c^2-1\right)\frac{\partial^2\mathcal{V}}{\partial z^2}+\left(c-c^3\right)\frac{\partial^2\mathcal{W}}{\partial z^2}=0; \tag{37}$$

and

$$j^2\left(c^2-1\right)\frac{\partial^2\mathcal{U}}{\partial z^2}-c^4\,\mathcal{U}+c\,(1-c^2)\frac{\partial\mathcal{V}}{\partial z}-c^2(c^2-2)\,\frac{\partial\mathcal{W}}{\partial z}-k=0, \tag{38}$$

respectively.

We construct the eigenvalue matrix for the above system of equations:

$$\begin{bmatrix} c^2 & c\,\lambda & \left(1-c^2\right)\,\lambda \\ \left(c^3-2\,c\right)\,\lambda & \left(c^2-1\right)\,\lambda^2 & \left(c-c^3\right)\,\lambda^2 \\ \left(c^2-1\right)j^2\,\lambda^2-c^4 & \left(c-c^3\right)\lambda & c^2\left(c^2-2\right)\lambda \end{bmatrix},$$

from which we obtain the eigenvalues as $\lambda = 0$ (with multiplicity 3), $\lambda = -i\,\nu$ and $\lambda = i\,\nu$, where $\nu = c\sqrt{2-c^2}/\left(1-c^2\right)\,j$.

Two of the solutions associated with $\lambda = 0$ are constants, $\mathcal{V} = v_{\rm con}$ (constant) and $\mathcal{W} = w_{\rm con}$ (constant). The last of these solutions takes the form $\mathcal{U} = u_{\rm lin}$, $\mathcal{V} = v_{\rm lin}\,z$, $\mathcal{W} = w_{\rm lin}\,z$, where $u_{\rm lin}$, $v_{\rm lin}$, and $w_{\rm lin}$ are constants. A solution of this type also generates the nonhomogeneous terms in the equations so we can solve these together. The solution is

$$u_{\rm lin} = -\frac{k+\left(c^2-1\right)c^2+r_1+2}{c^2}, \quad v_{\rm lin} = \frac{k+3\,c^4+\left(r_1-2\right)\,c^2}{c}, \quad w_{\rm lin} = r_1,$$

where r_1 is a constant of integration.

Now we find the harmonic component of the solution. We first consider the case where $\mathcal{U}$ is the cosine, and $\mathcal{V}$ and $\mathcal{W}$ are the sine components of the solution. These are of the form $\mathcal{U} = u_{\cos}\,\cos\nu z, \quad \mathcal{V} = v_{\sin}\,\sin\nu z, \quad \mathcal{W} = w_{\sin}\,\sin\nu z$. Using these in the associated homogeneous forms of (36) and (38) we find that

$$u_{\cos} = r_2, \quad v_{\sin} = \frac{2\,\left(c^2-1\right)\,j\,r_2}{\sqrt{2-c^2}}, \quad w_{\sin} = \frac{c\,j\,r_2}{\sqrt{2-c^2}},$$

where r_2 is a constant of integration. The proposed form of the solution is found to be consistent with the tangential force equation (37).

We next consider the case where $\mathcal{U}$ is the sine, and $\mathcal{V}$ and $\mathcal{W}$ are the cosine components of the solution. The proposed form of the solution is $\mathcal{U} = u_{\sin}\,\sin\nu z$, $\mathcal{V} = v_{\cos}\,\cos\nu z, \quad \mathcal{W} = w_{\cos}\,\cos\nu z$. By substituting these in the associated homogeneous forms of equations (36) and (38), and solving we obtain

$$u_{\sin} = r_3, \quad v_{\cos} = \frac{2\,\left(1-c^2\right)\,j\,r_3}{\sqrt{2-c^2}}, \quad w_{\cos} = -\frac{c\,j\,r_3}{\sqrt{2-c^2}},$$

where r_3 is a constant. The proposed form of the solution is also found to satisfy the tangential force equation (37).

We now use the various solutions obtained above to construct the general solution of the above system of equations:

$$\begin{aligned} \mathcal{U}(z) &= u_{lin} + u_{cos}\,\cos\nu z + u_{sin}\,\sin\nu z \\ \mathcal{V}(z) &= v_{con} + v_{lin}z + u_{cos}\,\cos\nu z + u_{sin}\,\sin\nu z \\ \mathcal{W}(z) &= w_{con} + w_{lin}z + u_{cos}\,\cos\nu z + u_{sin}\,\sin\nu z \end{aligned}$$

where r_1, r_2 and r_3 are constants and $\nu = c\sqrt{2-c^2}/\left(1-c^2\right)\,j$. Observing that v_{con} and w_{con} are both zero from the boundary conditions, the general solution is given as follows:

$$\begin{aligned} \mathcal{U}(z) &= -\tfrac{k+(3\,c^2-5)c^2+r_1+2}{c^2} + r_2\,\cos\nu z + r_3\,\sin\nu z \\ \mathcal{V}(z) &= \tfrac{k+3\,c^4+(r_1-2)\,c^2}{c}\,z - \tfrac{2\,(1-c^2)\,j}{\sqrt{2-c^2}}(r_2\,\sin\nu z - r_3\,\cos\nu z) \\ \mathcal{W}(z) &= r_1 z + \tfrac{c\,j}{\sqrt{2-c^2}}(r_2\,\sin\nu z - r_3\,\cos\nu z). \end{aligned} \tag{39}$$

Applying the boundary conditions $\mathcal{U}(\pm 1) = 0$, $\mathcal{V}(\pm 1) = 0$, $\mathcal{W}(\pm 1) = \pm 2$ we obtain the constants r_1, r_2, r_3, and k as

$$r_1 = \frac{j\left(c^2-2\right)\,\sin\nu + 2\,c\sqrt{2-c^2}\,\cos\nu}{j\,\left(1-c^2\right)\sin\nu - c\,\sqrt{2-c^2}\,\cos\nu},\; r_2 = \frac{c\,\sqrt{2-c^2}}{j\,\left(1-c^2\right)\sin\nu - c\sqrt{2-c^2}\,\cos\nu},$$

$$r_3 = 0, \quad \text{and} \quad k = \frac{c^2\left[(3\,c^4 - 8\,c^2 + 6)j\,\sin\nu + c\,\sqrt{2-c^2}\,\cos\nu\right]}{j\,\left(1-c^2\right)\sin\nu - c\,\sqrt{2-c^2}\,\cos\nu} \quad \text{respectively,}$$

where $\nu = c\,\sqrt{(2-c^2)}/(1-c^2)j$. With $e_0 = 3\,\cos^2\phi - 2 + e_i/\varepsilon$, we obtain $S_0(r) = 1$ and

$$j = \alpha\sqrt{\frac{\gamma^2-1}{2\,\ln(\gamma)}}.$$

The functions $\mathcal{U}(z)$, $\mathcal{V}(z)$ and $\mathcal{W}(z)$ represent the displacement of the collagen fibres when the disc bulges. The way the disc bulges, and the collagen fibres are displaced, depends on the value of j and their orientation with the horizontal plane before they are compressed. Assuming that the fibres have an average orientation of 30^o with respect to the horizontal plane, Figures 4, 5 and 6 illustrate respectively the radial, azimuthal and axial displacements of the fibres.

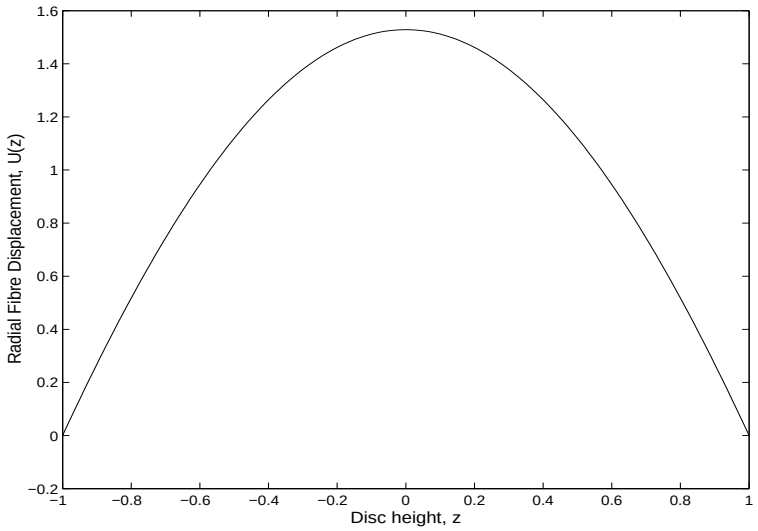

FIGURE 4. Radial fibre displacement with $\phi = 30^0$.

6. **Axial load and fluid pressure balances.** When the disc is loaded, the force transmitted through the vertebral/intervertebral disc interface can not be directly equated to the loading force. This is because the body has to balance the moment of forces on the spine as well as the force itself. It does this by providing additional forces through the action of muscles (and ligaments). There are no direct practical methods to measure the loads imposed on the spine and the forces experienced by the muscles as a result of different physical activities. These are indirectly inferred from measurements of intradiscal pressures.

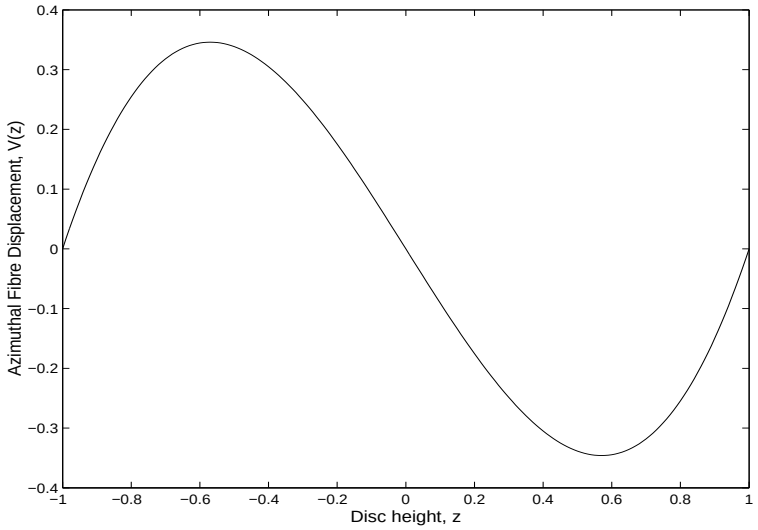

FIGURE 5. Azimuthal fibre displacement with $\phi = 30^0$.

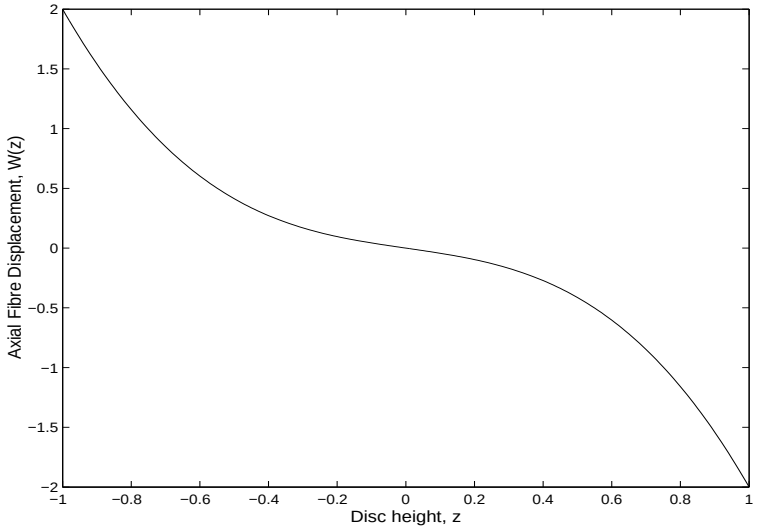

FIGURE 6. Axial fibre displacement with $\phi = 30^o$.

Firstly, the inward force generated by the fibres must be balanced by the outward effect of the pressure. We can express this as an equation using (14). This equation is valid in the initial as well as the final state, but in the initial state u, v and w are all zero and the equation reduces to the form

$$\frac{\partial P}{\partial r} = -\rho_i T(e_i) \frac{1}{r \sec\phi \tan\phi}. \tag{40}$$

On integrating with respect to r over $[a, b]$ and we obtain

$$\begin{aligned} P_i &= \frac{\cos^2\phi}{\sin\phi}\int_a^b \frac{\rho_i T(e_i)}{r}\,dr \\ &= \rho_i\, T(e_i)\frac{\cos^2\phi}{\sin\phi}\,\ln(\frac{b}{a}), \end{aligned} \tag{41}$$

where the first line is generally true and the second line follows when our assumption about the uniformity of e_i is correct. In the experiment of Andersson and Schultz [3] the pressure in the nucleus before injection is cited and substitution of this value in (41) enables us to determine the initial strain e_i.

Let W be the force that is transmitted directly through the intervertebral disc. Then W must be equal to the net force provided by the pressure and tension forces at the vertebra interface. Denoting the pressure in the nucleus by P_n, the balance of forces is given by

$$W = \pi a^2 P_n + (1-\eta)\int_a^b 2\pi P r\,dr - \int_a^b 2\pi\,\rho_i T r\sin\phi\,dr, \tag{42}$$

where η is the fibre volume fraction. The terms of the right hand side of the equation have the following interpretation:

- The first term is the pressure force of the nucleus pulposus.
- The second term is the pressure of the ground substance within the annulus. The factor $(1-\eta)$ allows for the volume taken up by the collagen fibres.
- The third term is the force resulting from the tension in the collagen fibre network. The $\sin\phi$ factor comes from taking the vertical component of the tension force.

Performing an integration by parts on the first integral in (42) and using the condition $P|_{r=b} = 0$, we get

$$W = \eta\,\pi\,a^2\,P_n - \pi(1-\eta)\int_a^b r^2\,\frac{\partial P}{\partial r}\,dr - 2\pi\,\sin\phi\int_a^b \rho_i T r\,dr, \tag{43}$$

where $P|_{r=a} = P_n$. The pressure gradient to zero order can be determined from equation (29), which in dimensional form is

$$\frac{\partial P}{\partial r} = -\frac{\cos^2\phi}{\sin\phi}\,\frac{\rho_i T}{r}. \tag{44}$$

On substitution of this in (43) we get

$$W = \eta\,\pi\,a^2\,P_n + \pi\,\frac{(1-\eta)\cos^2\phi - 2\,\sin^2\phi}{\sin\phi}\int_a^b \rho_i T\,r\,dr. \tag{45}$$

We had earlier assumed that the tension is uniform throughout the annulus. It is one of the simplest assumptions that we can make and allows convenient evaluation of the integrals. Our equations show that the tension is then uniform everywhere after displacement. The final result can then be expressed entirely in terms of P_n using the relation

$$P_n = \frac{\cos^2\phi}{\sin\phi}\,\rho_i T\ln(\gamma), \tag{46}$$

which follows from (41). Thus

$$W = \left[\eta\,a^2 + \frac{(1-\eta)\cos^2\phi - 2\,\sin^2\phi}{2\ln(\gamma)\,\cos^2\phi}\,(b^2-a^2)\right]\pi\,P_n.$$

In order to compare our predictions with experimental results, we rewrite the above equation in the form

$$W = \left[\frac{\eta}{\gamma^2} + \frac{(1-\eta)\cos^2\phi - 2\,\sin^2\phi}{2\ln(\gamma)\,\cos^2\phi}\,(1-\frac{1}{\gamma^2})\right]\pi\,b^2\,P_n, \tag{47}$$

where $\gamma = b/a$. Then $\pi\,b^2$ is the cross-sectional area of the disc so $\pi\,b^2\,P_n$ is the natural estimate of the loading force obtained by multiplying the total disc area by the nucleus pressure. The square bracket factor in front of this term expresses the reduction in the force due to the tapering off of the pressure in the annulus fibrosus and the opposing effect of the fibres. Taking the values $\eta = 0.16$ and $\gamma^2 = 2$, this factor can be evaluated and we find

$$W \simeq 0.205\,\pi\,b^2\,P_n. \tag{48}$$

The axial compressive load on a disc can thus be calculated from measured intradiscal pressures using this formula.

7. **Results and discussion.** The evaluation of loads upon the spine is quite a difficult task. The literature offers several conflicting estimates of axial load for the same posture [24, 25, 31]. Our belief is that the variation in the measurements is caused by the axial component of the forces in the muscles (and ligaments)that surround the spine. In most postures, especially flexion and extension, forces resulting from muscle activity are required to stabilize the spine. The compressive force down the axis of the spine is then due to the sum of the body weight and the tensile forces in the muscles.

In vivo studies show that intradiscal pressures increase with increasing load in all modes of loading but pressure increases due to flexion and lateral bending are significantly larger than those caused by either symmetric compression of the same magnitude or torsional moments [4]. Most of the existing experimental investigations have attempted to measure the increase in intradiscal pressure when the disc is loaded. Changes in intradiscal pressures associated with postural change have also been measured [6, 11]. Though experimental results suggest that the pressure in the disc is directly related to the compressive load on it, there has never been any explicit method to determine the load directly.

We will compare the model predictions with the results from two groups of experiments, one with the subject sitting and the second with the subject standing. Most of the experimental values are taken from Nachemson and Morris [25]. The fourth lumbar disc results reported in Table 1 is taken from Wilke et al. [36]. In their experiments Nachemson and Morris measured the pressure in the nucleus of the third and fourth lumbar discs for different loads held by the subject. They also estimated the body mass that was supported by the disc. The influence of posture was studied by measuring the intradiscal pressures in sitting and standing positions. The effect of added loads was determined with the subjects carrying weights of zero, 9.1 kg and 22.7 kg in their hands. They also estimated the body mass supported to be 26 kg at the third lumbar disc and 44.4 kg at the fourth lumbar disc. We use the units of measurement of Nachemson and Morris [25]: cm^2 for area, kg for load (weight) and kg/cm^2 for pressure.

By using the intradiscal pressure measurements (P_n) in [25] and applying equation (47), we predict the load on the disc under consideration. Our findings are given in Table 1. The 'Net Load'denotes the sum of the Load and body mass. The

last two columns of the table indicates whether the angle $\phi = 30^o$ or $\phi = 25^o$ has been used in the calculation.

TABLE 1. Load predictions in sitting position with and without added external load at $\phi = 30^o$ and $\phi = 25^o$

Disc	Load	P_n	Net load	W_{30}	W_{25}
Third lumbar disc	None	10.4	26.0	28.4	51.7
Cross-section area = 13.3 cm^2	9.1	15.3	35.1	41.7	76.0
Load above = 26 kg	22.7	23.3	48.7	63.5	115.7
Fourth lumbar disc	None	9.9	44.4	43.8	79.9
Cross-sectional area = 21.6 cm^2	9.1	12.7	53.5	56.2	102.5
Load above = 44.4 kg	22.7	17.1	67.1	75.7	138.0

In situations where the muscles apply no additional stresses to the spine one would expect the predicted load W to equal the Net Load. Using the commonly accepted angle of $\phi = 30^o$ (column W_{30}) we find that there is excellent agreement when there is no loading or light loading. As the load increases, however, the predicted load rises significantly above the Net Load. This is to be expected since a load of 22.7 kg is likely to produce significant stress in the muscles, even with the body in a seated position.

In the final column of Table 1 we have calculated W with $\phi = 25^o$. It is noticeable that W_{25} significantly exceeds W_{30} and the agreement with the Net Load is very poor. This result has been given to illustrate the strong sensitivity of W to the value of ϕ. This should be borne in mine since it is unlikely that the value of ϕ is exactly equal to 30^o in practice. A slightly larger value for ϕ could even improve the fit with the Net Load. However, ϕ has not be determined with such precision. Indeed it seems quite possible from the variation observed in experiments that ϕ varies from specimen to specimen.

A similar comparison of Net and predicted loads are made in Table 2 where the data is again for the third and fourth lumbar discs but with more than one subject and now in a standing position.

TABLE 2. Load predictions in standing position with and without added external load at $\phi = 30^o$

Disc	Load	Disc area	P_n	Net load	W_{30}
Third lumbar disc	None	19.9	7.4	47.5	30.2
	None	13.8	9.6	43.3	27.2
	None	15.7	8.2	36.5	26.4
(Nachemson & Morris [25])	None	20.6	10.9	53.2	46.0
Fourth lumbar disc	None	17.8	8.8	39.2	32.1
(Nachemson & Morris [25])	None	21.6	8.6	44.4	38.1
Fourth lumbar disc	None	18.0	5.1	m.	18.8
(Wilke *et al.* [36])	19.8	18.0	17.5	19.8+m	64.6

Here we find inconsistency for many of the load predictions. The effect of muscle action can only increase the nucleus pressure and so lead to a load prediction that

is in excess of the weight that is supported by the spine. Many of our predicted loads, however, are significantly less than the experimentally applied load, which should not be possible.

A possible explanation of this is that the experimental results of Nachemson and Morris may have been in error. Althoff *et al.* [2] performed a series of experiments (but whose results are in a form that we were not able to use) and reported that their results were considerably higher than those of Nachemson and Morris in the standing position. If the correct pressure values are the higher measured readings then this would lead to a larger load prediction and so could explain the discrepancy.

Model predictions based on the experimental results of Wilke *et al.* [36] for the fourth lumbar disc are presented at the bottom of Table 2. However, they made no estimates of the lumbar compressive forces (loads) in their study. So an unknown estimate, denoted by m, has been entered in the table. Note that if we assume that $m = 18.8\,\text{kg}$ (so that the first readings are in agreement) then the predicted load for the second measurement is in excess of the Net Load, which is consistent with our model interpretation that excess loading can occur through muscle activity.

8. **Conclusion.** A model of an intervertebral disc has been developed in which the annulus fibrosus is represented as a series of fibre sheets separated by liquid-like layers of ground substance. Thus it does not behave as a rigid composite. The model has been applied to predict the compressive loads on a disc in both sitting and standing positions with and without additional external loads. In spite of the many assumptions and simplifications made in formulating the analytical model, results are found to be in agreement with estimated compressive forces on the disc for data from seated subjects by Nachemson and Morris [25]. There is poor agreement with data from standing subjects but other literature sources (Althoff *et al.* [2]) have stated that the experimental measurements were in error for this case. Our results are consistent with the results of Wilke *et al.* [36].

Acknowledgments. We would like to thank Dr Alan Jones very much for his valuable comments and suggestions.

REFERENCES

[1] M. A. Adams and W. C. Hutton, *Mechanics of the intervertebral disc*, in "The Biology of the Intervertebral Disc" (ed. P. Ghosh), **II**, CRC Press, Inc., Boca Raton, Florida, (1988), 40–69.

[2] I. Althoff, P. Brinckmann, W. Frobin, J. Sandover and K. Burton, *An improved method of stature measurement for quantitative determination of spinal loading. Application of sitting postures and whole body vibration*, Spine, **17** (1992), 682–693.

[3] G. B. J. Andersson and A. B. Schultz, *Effects of fluid injection on mechanical properties of intervertebral discs*, J. Biomechanics, **12** (1979), 453–458.

[4] G. B. J. Andersson and A. Nachemson, *Intradiskal pressure, intra-abdominal pressure and myoelectric back muscle activity related to posture and loading*, Clin. Orthop., **129** (1977), 156–164.

[5] B. A. Best, F. Guilak, L. A. Setton, W. Zhu, F. Saed-Nejad, A. Ratcliffe, M. Weidenbaum and V. C. Mow, *Compressive mechanical properties of the human annulus fibrosus and their relationship to biochemical composition*, Spine, **19** (1994), 212–221.

[6] M. T. Bayliss, B. Johnstone and J. P. O'brien, *Poteoglycan systhesis in the human intervertebral disc: Variation with age, region and pathology*, Spine, **13** (1988), 972–981.

[7] M. T. Bayliss and B. Johnstone, *Biochemistry of the intervertebral disc*, in "The Lumbar Spine and Back Pain" (ed. M.I.V. Jayson), Longman Group UK Limited, 1992.

[8] T. B. Belytschko, R. F. Kulak, A. B. Schultz and J. D. Galante, *Finite element stress analysis of an intervertebral disc*, J. Biomechanics, **7** (1974), 277–285.

[9] S. Bernick and R. Caillet, *Vertebral end–plate changes with ageing of human vertebrae*, Spine, **7** (1982), 97–102.

[10] P. Brinckmann and H. Grootenboer, *Change of disc height, radial disc bulge, and intradiscal pressure from discectomy: An in vitro investigation on human lumbar discs*, Spine, **16** (1991), 641–646.

[11] P. Dolan, M. Earley and M. A. Adams, *Bending and compressive stresses on the lumbar spine during lifting activities*, J. Biomechanics, **27** (1994), 1237–1248.

[12] Wu Han-Chin and Yao Ren-Feng, *Mechanical behaviour of the human annulus fibrosus*, J. Biomechanics, **9** (1976), 1–7.

[13] A. D. Holmes, D. W. L. Hukins and A. J. Freemont, *End-plate displacement during compression of lumbar vertebra-disc-vertebra segments and the mechanism of failure*, Spine, **18** (1993), 128–135.

[14] D. W. L. Hukins, *Disc structure and function*, in "The Biology of the Intervertebral Disc" (ed. P Ghosh), **I**, CRC Press, Inc., Boca Raton, Florida, (1988), 1–37.

[15] M. D. Humzah and R. W. Soames, *Human intervertebral disc: Structure and function*, The Anatomical Record, **220** (1988), 337–356.

[16] H. Inoue and T. Takeda, *Three dimensional observation of collagen framework of intervertebral discs*, Acta Orthopaedica Scandinavica, **46** (1975), 949–956.

[17] H. Ishihara, D. S. McNally, J. P. G. Urban and A. C. Hall, *Effects of hydrostatic pressure on matrix synthesis in different regions of the intervertebral disc*, J. Applied Physiology, **80** (1996), 339–346.

[18] R. F. Kulak, T. B. Belytschko and A. B. Schultz, *Nonlinear behaviour of the human intervertebral disc under axial loading*, J. Biomechanics, **9** (1976), 377–386.

[19] M. Y. Lu, C. W. Hutton and M. V. Gharpuray, *Can variations in intervertebral disc height affect the mechanical function of the disc?*, Spine, **21** (1996), 2208–2217.

[20] F. Marchand and A. M. Ahmed, *Investigation of the laminate structure of lumbar disc annulus fibrosus*, Spine, **15** (1990), 402–410.

[21] R. M. H. McMinn, "Last's Anatomy: Regional and Applied," 9^{th} edition, Churchill Livingstone, (1994), pp. 537.

[22] D. S. McNally and M. A. Adams, *Internal intervertebral disc mechanics as revealed by stress profilometry*, Spine, **17** (1992), 66–73.

[23] A. Nachemson, *Lumbar mechanics as revealed by lumbar intradiscal pressure measurements*, in "The Lumbar Spine and Back Pain" (ed. M. I. V. Jayson), Longman Group UK Limited, 1992.

[24] A. Nachemson and G. Elfstrom, *Intravital dynamic pressure measurements in lumbar discs. A study of common movements, maneuvers and exercises*, Scand. J. Rehab. (Suppl.), **1** (1970), 1–40.

[25] A. Nachemson and J. M. Morris, *In vivo measurements of intradiscal pressure*, J. Bone Jt Surg, **46A** (1964), 1077–1092.

[26] R. N. Natarajan, J. H. Ke and G. B. J. Andersson, *A model to study the disc degeneration process*, Spine, **19** (1994), 259–265.

[27] Matthias Ngwa, "Stress-Strain Problems in Biological Systems," Ph.D thesis, The University of Manchester, UK, 2003.

[28] N. D. Panagiotacopulos, M. H. Pope, R. Bloch and M. H. Krag, *Water content in human intervertebral discs. Part II: Viscoelastic behaviour*, Spine, **12** (1987), 918–924.

[29] H. S. Ranu, R. A. Denton and A. I. King, *Pressure distribution under an intervertebral disc - an experimental study*, J. Biomechanics, **12** (1979), 807–812.

[30] M. Reuber, A. Schultz, F. Denis and D. Spencer, *Bulging of lumbar intervertebral disks*, J. Biomech. Eng., **104** (1982), 187–192.

[31] A. Schultz, G. Andersson, R. Ortengren, K. Haderspeck and A. Nachemson, *Loads on the lumbar spine. Validation of a biomechanical analysis by measurements of intradiscal pressures and myoelectric signals*, J. Bone Joint Surg., **64** (1982), 713–720.

[32] R. S. Snell, "Clinical Anatomy for Medical Students," 6^{th} edition, Lippincott William and Wilkins, (2000), 817–828.

[33] R. L. Spilker, *Mechanical behaviour of a simple model of an intervertebral disc under compressive loading*, J. Biomechanics, **13** (1980), 895–901.

[34] R. L. Spilker, D. M. Daugirda and A. B. Shultz, *Mechanical response of a simple finite element model of the intervertebral disc under complex loading*, J. Biomechanics, **17** (1984), 103–112.

[35] K. G. Vijay and J. N. Weinstein, "Biomechanics of the Spine: Clinical and Surgical Perspective," CRC Press, Boca Raton, 1990.
[36] H. J. Wilke, P. Neef, T. Hoogland and L. E. Claes, *New In vivo measurements of pressures in the intervertebral disc in daily life*, Spine, **24** (1999), 775–762.

Appendix - The force balance equations. Here we show how equations (15) and (16) were derived from the raw form of the force equations. The main problem is the expression of the final coordinate system $(R,\,\Theta,\,Z)$ with its associated coordinate basis, $(\hat{\mathbf{R}},\hat{\mathbf{\Theta}},\mathbf{k})$, in terms of the original coordinate frame $(r,\,\theta,\,z)$ and the displacement fields $(u,\,v,\,w)$.

The tangential force equation. We begin by converting (11). A typical fibre point in its displaced location has position vector $\mathbf{X} = R\hat{\mathbf{R}} + Z\mathbf{k}$ where the coordinates $(R,\,\Theta,\,Z)$ are given in (2). Then a tangent vector to the displaced fibre is given by

$$\begin{aligned}\mathbf{t} &= \frac{\partial \mathbf{X}}{\partial s} = \frac{\partial R}{\partial s}\hat{\mathbf{R}} + R\frac{\partial \Theta}{\partial s}\hat{\mathbf{\Theta}} + \frac{\partial Z}{\partial s}\mathbf{k}\\ &= q\tan\phi\, u_z^*\,\hat{\mathbf{R}} + (q+u^*)(1+q\tan\phi\, v_z^*)\hat{\mathbf{\Theta}} + q\tan\phi\,(1+w_z^*)\,\mathbf{k}, \qquad \text{(A-1)}\end{aligned}$$

where the asterisk denotes that the quantity is being evaluated at $(q, qs\tan\phi)$. The final equation is an identity which is true for all values of q and s, and remains true if we replace $q \to r$, $qs\tan\phi \to z$. This also holds in subsequent equations to be derived. The asterisk is therefore unnecessary in the final form of any derived equation and will be omitted henceforth.

From the above equation it follows that

$$\begin{aligned}|\mathbf{t}| &= \left\{u_z^{*2}q^2\tan^2\phi + (q+u^*)^2(1+v_z^*q\tan\phi)^2 + (1+w_z^*)^2q^2\tan^2\phi\right\}^{\frac{1}{2}},\\ &= \left|\frac{d\mathbf{X}}{ds}\right| = \frac{dl}{ds}. \qquad \text{(A-2)}\end{aligned}$$

This can be used in turn to calculate a unit tangent,

$$\hat{\mathbf{t}} = \frac{\mathbf{t}}{|\mathbf{t}|} = \frac{1}{dl/ds}\mathbf{t}. \qquad \text{(A-3)}$$

A normal to the plane of the sheet can be calculated by the following argument. Consider two adjacent points on the same displaced sheet with the same Θ- coordinate. Let these be (R,Θ,Z) and $(R+dR,\Theta,Z+dZ)$. Then a normal will be given by a multiple of $-dZ\,\hat{\mathbf{R}} + dR\,\mathbf{k}$. Now these points originally lay at (r,θ,z) and $(r,\theta+d\theta,z+dz)$. They had the same radial value r, since they lay on the same sheet but they had distinct values of θ and z. Because of the axial symmetry the displaced value of θ is irrelevant for the calculation of the normal, but the displacement dz is relevant. From the displacement mapping we know that $R+dR = r + u(r,z+dz)$ and $Z+dZ = z+dz+w(r,z+dz)$. From these we can find expressions for dR and dZ, and so (cancelling the dz factor) deduce that

$$\mathbf{n} = -(1+w_z)\hat{\mathbf{R}} + u_z\mathbf{k}. \qquad \text{(A-4)}$$

The unit normal can then be found by dividing by the modulus of this vector.

$$\hat{\mathbf{n}} = \frac{1}{N}\left\{-(1+w_z)\hat{\mathbf{R}} + u_z\mathbf{k}\right\}, \qquad \text{(A-5)}$$

where $N = |\hat{\mathbf{n}}| = \{1 + 2w_z + w_z^2 + u_z^2\}^{\frac{1}{2}}$. We now calculate $\hat{\mathbf{b}}$ from its definition as $\hat{\mathbf{b}} = \hat{\mathbf{t}} \wedge \hat{\mathbf{n}}$.

$$\begin{aligned}\hat{\mathbf{b}} &= F\{u_z(r+u)(1+r\tan\phi\, v_z)\hat{\mathbf{R}} - [(1+w_z)^2 + u_z^2]\, q\tan\phi\,\hat{\boldsymbol{\Theta}} \\ &\qquad + (1+w_z)(r+u)(1+r\tan\phi\, v_z)\mathbf{k}\}, \end{aligned} \tag{A-6}$$

where F (eventually irrelevant) is a scalar factor, $F = 1/[N(dl/ds)]$. We are now in a position to obtain the final form of (11). First we write it as

$$\frac{1}{dl/ds}\frac{\partial \hat{\mathbf{t}}}{\partial s}.\hat{\mathbf{b}} = 0. \tag{A-7}$$

From (A-3) we deduce that

$$\frac{\partial \hat{\mathbf{t}}}{\partial s} = \frac{1}{dl/ds}\frac{\partial \mathbf{t}}{\partial s} - \frac{\partial}{\partial s}\left(\frac{1}{dl/ds}\right)\mathbf{t}. \tag{A-8}$$

However, $\mathbf{t}$ is perpendicular to $\mathbf{b}$ so when this is substituted into (A-7) the dot product with the second term of (A-8) equals zero and so (A-7) reduces to

$$\frac{\partial \mathbf{t}}{\partial s}.\hat{\mathbf{b}} = 0. \tag{A-9}$$

From (A-1) we find

$$\begin{aligned}\frac{\partial \mathbf{t}}{\partial s} &= [r^2\tan^2\phi\, u_{zz} - (r+u)(1+r\tan\phi\, v_z)^2]\,\hat{\mathbf{R}} \\ &\quad + [2r\tan\phi\, u_z(1+r\tan\phi\, v_z) + r^2\tan^2\phi(r+u)v_{zz}]\,\hat{\boldsymbol{\Theta}} \\ &\quad + r^2\tan^2\phi\, w_{zz}\mathbf{k}, \end{aligned} \tag{A-10}$$

where we have used

$$\frac{\partial \hat{\mathbf{R}}}{\partial s} = \frac{\partial \Theta}{\partial s}\hat{\boldsymbol{\Theta}} = (1+q\tan\phi\, v_z)\hat{\boldsymbol{\Theta}}, \quad \frac{\partial \hat{\boldsymbol{\Theta}}}{\partial s} = -\frac{\partial \Theta}{\partial s}\hat{\mathbf{R}} = -(1+q\tan\phi\, v_z)\hat{\mathbf{R}}.$$

We now substitute (A-6) and (A-10) into (A-9) and take the dot product to obtain

$$\begin{aligned}&r^2\tan^2\phi(r+u)(1+w_z)(1+r\tan\phi\, v_z)w_{zz} - (r+u)^2(1+r\tan\phi\, v_z)^3 u_z \\ &-r^2\tan^2\phi\,[(1+w_z)^2 + u_z^2]\,[2u_z(1+r\tan\phi\, v_z) + r\tan\phi(r+u)v_{zz}] \\ &+r^2\tan^2\phi(r+u)(1+r\tan\phi\, v_z)u_z u_{zz} = 0. \end{aligned} \tag{A-11}$$

The radial force equation. In this section we express (14) in terms of the displacement fields. We begin by converting the derivative with respect to R on the left hand side of the equation into derivatives with respect to the original co-ordinate system, (r, θ, z):

$$\frac{\partial P}{\partial R} = \frac{\partial P}{\partial r}\frac{\partial r}{\partial R} + \frac{\partial P}{\partial z}\frac{\partial z}{\partial R}.$$

By differentiating the identities

$$R = r + u(r,z), \qquad Z = z + w(r,z)$$

with respect to R and Z we obtain four equations which may be solved to obtain expressions for the partial derivatives of r and z. In particular,

$$\frac{\partial r}{\partial R} = \frac{1+w_z}{D}, \qquad \frac{\partial z}{\partial R} = -\frac{w_r}{D}, \tag{A-12}$$

where

$$D = 1 + (u_z + w_z) + (u_r w_z - u_z w_r).$$

Next we find an expression for ρ_s in terms of $\rho_s^{(0)}$, where $\rho_s^{(0)}$ is the equivalent linear density in the initial configuration of a sheet, i.e., the number of fibres per unit length that pass through a circular arc of constant (r, z) within the sheet. Consider such an arc that initially extends between θ_1 and θ_2. After displacement this will still be a circular arc subtending the same angle $\theta_2 - \theta_1$, but with a different radius, $r + u(r, z)$. The vertical co-ordinate is also different, but this does not affect the calculation. The number of fibres passing through each arc is the same, so

$$\rho_s^{(0)} \left[r(\theta_2 - \theta_1) \right] = \rho_s \left[(r + u)(\theta_2 - \theta_1) \right].$$

It then follows that

$$\rho_s = \rho_s^{(0)} \frac{r}{r + u}.$$

We shall assume that $\rho_s^{(0)}$ is a constant, i.e., the fibres have the same constant spacing in any sheet. For this to be so, more fibres must be present in the outer (larger radius) sheets.

Next we calculate ρ_R in terms of $\rho_r^{(0)}$, where $\rho_r^{(0)}$ is the equivalent linear density in the original configuration, i.e., the number of sheets per unit length that pass through a radial line of constant (θ, z). Consider an element of a radial line in the final configuration that extends from (R, Θ, Z) to $(R + dR, \Theta, Z)$. The number of sheets intersecting this line is $\rho_R dR$. Now consider the original line element that transformed into this line element after displacement. The endpoints of the original element lie at (r, θ, z) and $(r + dr, \theta + d\theta, z + dz)$. Now we need to find an expression for the number of sheets that cross between the two original end points. The path chosen for this is irrelevant. Thus we may choose the path to first go from (r, θ, z) to $(r + dr, \theta, z)$, during which it crosses $\rho_r^{(0)} dr$ sheets, and from there to $(r + dr, \theta + d\theta, z + dz)$, during which it crosses no sheet (since they are all vertical circular cylinders in the original configuration). The number of sheets is the same for the initial and final configurations, so it follows that

$$\rho_R dR = \rho_r^{(0)} dr = \rho_r^{(0)} \frac{\partial r}{\partial R} dR.$$

Thus from (A-12), we have

$$\rho_R = \rho_r^{(0)} \frac{1 + w_z}{D}.$$

We shall assume that $\rho_r^{(0)}$ is a constant, i.e. that sheets are originally spaced at fixed intervals as we move outward through the disc.

Next we derive an expression for $\sin \Phi$. We can obtain $\cos \Phi$ by taking the dot product of the azimuthal vector $\hat{\boldsymbol{\Theta}}$ with the unit tangent $\hat{\mathbf{t}}$ along a fibre. The unit tangent was calculated earlier and its formula is given by (A-1), (A-2) and (A-3). From these we find that

$$\sin \Phi \quad = \quad \sqrt{1 - \cos^2 \Phi} = \frac{N r \tan \phi}{dl/ds}.$$

Next we derive an expression for $(\partial \hat{\mathbf{t}}/\partial l) \cdot \hat{\mathbf{n}}$. The separate parts are given by (A-5) and (A-8). We note that an expression for the final term in (A-8) is not

required since $\mathbf{t}$ is perpendicular to $\hat{\mathbf{n}}$. Thus

$$\begin{aligned}\frac{\partial \hat{\mathbf{t}}}{\partial l}.\hat{\mathbf{n}} &= \frac{1}{dl/ds}\frac{\partial \mathbf{t}}{\partial s}.\hat{\mathbf{n}} \\ &= \frac{1}{N(dl/ds)}\left\{(1+w_z)\left[(r+u)(1+r\tan\phi\, v_z)^2\right.\right. \\ &\qquad \left.\left. - r^2\tan^2\phi\, u_{zz}\right] + r^2\tan^2\phi\, u_z w_{zz}\right\} \qquad \text{(A-13)}\end{aligned}$$

Finally we define $\rho_i = \rho_r^{(0)}\,\rho_s^{(0)}$. Substituting all these results in (14) we obtain the radial component of the force balance equation as

$$(1+w_z)\frac{\partial P}{\partial r} - w_r\frac{\partial P}{\partial z} = -\rho_i\, S(e)\frac{(1+w_z)}{(r+u)(dl/ds)N^2\tan\phi}\times \qquad \text{(A-14)}$$

$$\left\{(1+w_z)\left[(r+u)(1+r\tan\phi\, v_z) - r^2\tan^2\phi\, u_{zz}\right] + r^2\tan^2\phi\, u_z w_{zz}\right\}.$$

Received January 17, 2010; Accepted April 8, 2011.

E-mail address: eoasma@rit.edu
E-mail address: mangwa@cbe.ab.ca